

## **Synthesis of multiple-free plane-wave responses**

Giovanni Angelo Meles, Lele Zhang, Jan Thorbecke, Kees Wapenaar and Evert Slob

Department of Geoscience and Engineering, Delft University of Technology, Stevinweg 1, 2628 CN Delft, The Netherlands  
G.A.Meles@tudelft.nl

### **Abstract**

Seismic images provided by Reverse Time Migration can be contaminated by artefacts associated with the migration of multiples. Multiples can corrupt seismic images producing both false positives, i.e. by focusing energy at unphysical interfaces, and false negatives, i.e. by destructively interfering with primaries. Multiple prediction / primary synthesis methods are usually designed to operate on point source gathers, and can therefore be computationally demanding when large problems are considered. Here, a new scheme is presented for fully data-driven retrieval of primary responses to plane-wave sources. The proposed scheme, based on convolutions and cross-correlations of the reflection response with itself, extends a recently devised point-sources primary retrieval method for to plane-wave source data. As a result, the presented algorithm allows fully data-driven synthesis of primary reflections associated with plane-wave source data. Once primary plane-wave responses are estimated, they are used for multiple-free imaging via standard reverse time migration.

## Introduction

Most standard imaging methods are based on linear (Born) approximations, for which multiply scattered waves represent a source of coherent noise. Multiple-related artefacts can be dealt with via Marchenko redatuming methods. Marchenko redatuming estimates Green's functions between arbitrary locations inside a medium and real receivers located at the surface (Wapenaar et al. (2014)). Despite its requirements on the quality of the reflection data, the Marchenko scheme has already been successfully applied to field data (Ravasi et al. (2016); Staring et al. (2018)). Recent advances in Marchenko methods led to revised derivations which resulted in fully data driven demultiple / primary synthesis algorithms (van der Neut and Wapenaar (2016); Zhang et al. (2019); Zhang and Slob (2020)). In these revised derivations focusing properties are exploited in the data at the surface rather than in the subsurface. Following a similar approach to what inspired recent research on plane wave Marchenko redatuming (Meles et al. (2018)), we extend this newly introduced primary synthesis scheme, originally derived for point sources, to plane-wave sources.

## Theory

To derive their primary synthesis scheme, Zhang et al. (2019) exploited properties of the projected focusing functions  $v^-$  and  $v_m^+$  (van der Neut and Wapenaar (2016)), which satisfy the following equations:

$$\tilde{v}^-(\mathbf{x}'_0, \mathbf{x}''_0, t, t_2) = (\Theta_\varepsilon^{t_2+\varepsilon} R + \Theta_\varepsilon^{t_2+\varepsilon} \mathbf{R} v_m^+) (\mathbf{x}'_0, \mathbf{x}''_0, t) \text{ and } v_m^+(\mathbf{x}'_0, \mathbf{x}''_0, t, t_2) = (\Theta_\varepsilon^{t_2+\varepsilon} \mathbf{R}^* v^-) (\mathbf{x}'_0, \mathbf{x}''_0, t), \quad (1)$$

where  $\mathbf{R}$  indicates a convolution integral operator of the measured data with any wavefield, the superscript  $\star$  indicates time-reversal and  $\Theta_\varepsilon^{t_2+\varepsilon}$  is a muting operator removing values outside of the interval  $(\varepsilon, t_2 + \varepsilon)$ , where  $t_2$  is a two-way travelttime from a potential surface point and back to the surface and  $\varepsilon$  is a positive number to account for the finite bandwidth of the projected focusing functions. Terms in Eq. 1 are rearranged to get:

$$(I - \Theta_\varepsilon^{t_2+\varepsilon} \mathbf{R} \Theta_\varepsilon^{t_2+\varepsilon} \mathbf{R}^*) v^-(\mathbf{x}'_0, \mathbf{x}''_0, t, t_2) = \Theta_\varepsilon^{t_2+\varepsilon} R (\mathbf{x}'_0, \mathbf{x}''_0, t), \quad (2)$$

which, under standard convergence conditions, is solved by:

$$v^-(\mathbf{x}'_0, \mathbf{x}''_0, t, t_2) = \Theta_\varepsilon^{t_2+\varepsilon} R (\mathbf{x}'_0, \mathbf{x}''_0, t) + \left[ \sum_{M=1}^{\infty} (\Theta_\varepsilon^{t_2+\varepsilon} \mathbf{R} \Theta_\varepsilon^{t_2+\varepsilon} \mathbf{R}^*)^M \Theta_\varepsilon^{t_2+\varepsilon} R \right] (\mathbf{x}'_0, \mathbf{x}''_0, t). \quad (3)$$

This procedure allows to retrieve  $v^-(\mathbf{x}'_0, \mathbf{x}''_0, t, t_2)$ , whose last event, when its two-way travel time is  $t_2$ , is a transmission loss compensated primary reflection in  $R(\mathbf{x}'_0, \mathbf{x}''_0, t)$  (Zhang et al. (2019)). Instead of computing  $t_2$  as the two-way travelttime, we evaluate Eq. 3 for all possible values  $t_2$  and store results at  $t = t_2$ . In this way the (transmission-compensated) primary reflection response in  $R(\mathbf{x}'_0, \mathbf{x}''_0, t)$  is then fully retrieved. Here, following a similar approach to what was recently proposed to extend Marchenko redatuming from point-source to plane-wave concepts (Meles et al. (2018)), we consider integral representations of the projected focusing functions  $v^-$  and  $v_m^+$ . More precisely, we first define new projected focusing functions  $V^-(\mathbf{x}'_0, t)$  and  $V_m^+(\mathbf{x}'_0, t)$  as:

$$V^-(\mathbf{x}'_0, t, t_2) \equiv \int_{\partial D_0} d\mathbf{x}''_0 v^-(\mathbf{x}'_0, \mathbf{x}''_0, t, t_2), \text{ and } V_m^+(\mathbf{x}'_0, t, t_2) \equiv \int_{\partial D_0} d\mathbf{x}''_0 v_m^+(\mathbf{x}'_0, \mathbf{x}''_0, t, t_2). \quad (4)$$

Using again the time-domain formalism used above we can write:

$$V^-(\mathbf{x}'_0, t, t_2) = (\Theta_\varepsilon^{t_2+\varepsilon} R_{PW} + \Theta_\varepsilon^{t_2+\varepsilon} \mathbf{R} V_m^+) (\mathbf{x}'_0, t, t_2) \text{ and } V_m^+(\mathbf{x}'_0, t) = (\Theta_\varepsilon^{t_2+\varepsilon} \mathbf{R}^* V^-) (\mathbf{x}'_0, t) \quad (5)$$

where  $R_{PW}(\mathbf{x}'_0, t) \equiv \int_{\partial D_0} d\mathbf{x}''_0 R(\mathbf{x}'_0, \mathbf{x}''_0, t)$  is by definition the plane-wave source response of the medium. Following the same procedure discussed above, we can combine terms in equations 5 to get:

$$(I - \Theta_\varepsilon^{t_2+\varepsilon} \mathbf{R} \Theta_\varepsilon^{t_2+\varepsilon} \mathbf{R}^*) V^-(\mathbf{x}'_0, t, t_2) = \Theta_\varepsilon^{t_2+\varepsilon} R_{PW}(\mathbf{x}'_0, t) \quad (6)$$

which is solved by:

$$V^-(\mathbf{x}'_0, t, t_2) = \Theta_\varepsilon^{t_2+\varepsilon} R_{\text{PW}}(\mathbf{x}'_0, t) + \left[ \sum_{M=1}^{\infty} (\Theta_\varepsilon^{t_2+\varepsilon} \mathbf{R} \Theta_\varepsilon^{t_2+\varepsilon} \mathbf{R}^*)^M \Theta_\varepsilon^{t_2+\varepsilon} R_{\text{PW}} \right] (\mathbf{x}'_0, t) \quad (7)$$

This procedure allows to retrieve  $V^-(\mathbf{x}'_0, t)$ , whose last event, when its two-way travel time is  $t_2$ , is a transmission loss compensated primary reflection in  $R_{\text{PW}}(\mathbf{x}'_0, t)$ . By computing Eq. 7 for all possible values  $t_2$  and storing results at  $t = t_2$ , the (transmission-compensated) primary reflection response in  $R_{\text{PW}}(\mathbf{x}'_0, t)$  is then fully retrieved. Note that the process discussed here is totally data driven, and it is implemented by inversion of a family of linear operators, i.e.  $(I - \Theta_\varepsilon^{t_2+\varepsilon} \mathbf{R} \Theta_\varepsilon^{t_2+\varepsilon} \mathbf{R}^*)$ . Each value of  $t_2$  defines a different operator. Since these operators are linear and do not depend on the specific gather it is applied to, any linear combination of datasets can be processed at once, provided that all the corresponding sources are fired at the *same* time. When dipping plane waves, associated with point gathers fired at *different* times, are considered, we heuristically propose to extend 7 as:

$$V_{\text{DW}}^-(\mathbf{x}'_0, t, t_2) = \tilde{\Theta}_\varepsilon^{t_2+\varepsilon} R_{\text{DW}}(\mathbf{x}'_0, t) + \left[ \sum_{M=1}^{\infty} (\tilde{\Theta}_\varepsilon^{t_2+\varepsilon} \mathbf{R} \tilde{\Theta}_\varepsilon^{t_2+\varepsilon} \mathbf{R}^*)^M \tilde{\Theta}_\varepsilon^{t_2+\varepsilon} R_{\text{DW}} \right] (\mathbf{x}'_0, t) \quad (8)$$

where  $R_{\text{DW}}$  is the reflection response associated with a dipping plane wave source, and the upper and lower limits of the muting operators  $\tilde{\Theta}_\varepsilon^{t_2+\varepsilon}$  are parallel to the source input itself (see Fig. 1). The last event in  $V_{\text{DW}}^-(\mathbf{x}'_0, t, t_2)$ , when its two-way travel time equals the lower limit of the window  $\tilde{\Theta}_\varepsilon^{t_2+\varepsilon}$ , is then taken, in analogy to Eq. 7, as a transmission loss compensated primary reflection in  $R_{\text{DW}}(\mathbf{x}'_0, t)$ .

## Results

For our numerical experiment we consider a 2D model with dipping interfaces (Fig. 2(a)). The full dataset associated with 3 representative plane-wave sources fired at the surface of the model are shown in Figs. 2(b-d). Due to the strong impedance variations the data are contaminated with many internal multiples, as indicated by red arrows. We then apply to this dataset the primaries synthesis method as described in the section above. More precisely, we compute  $V^-$  and  $V_{\text{DW}}^-$  via Eqs. 7 and 8, respectively, for all values  $t_2$ , and by storing results at  $t = t_2$  we build parallel datasets, which theoretically only include primaries. The results of this procedure are shown in Figs. 2(e-g), with green arrows pointing at primaries barely visible in the full data-sets. Note that the algorithm is fully data driven, and no model information whatsoever nor any human intervention (e.g., picking) is involved in the process.

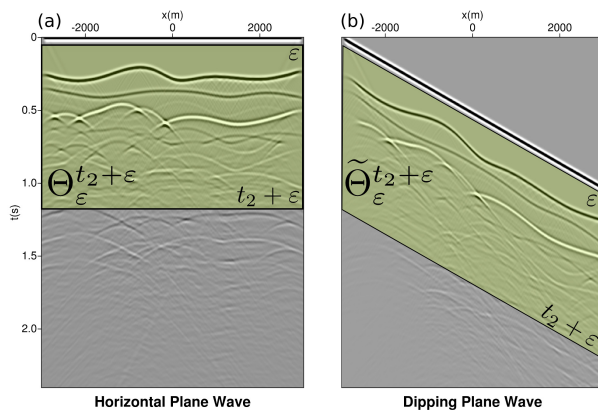


**Figure 1** The shaded green areas show the support of representative muting operators for horizontal ( $\Theta$  in (a)) and dipping ( $\tilde{\Theta}$  in (b)) plane wave sources (the corresponding data are shown in the background).

We apply the method to a total of 15 plane wave datasets (uniformly ranging from  $-35^\circ$  to  $35^\circ$ ) and stack the corresponding Reverse Time Migration images. Migration results are shown in Fig. 3. When the full plane-wave datasets are migrated, internal multiples contaminate the image, producing many false positive artefacts (indicated by red arrows in Fig. 3(a)). The image is much cleaner when the plane-wave primary gathers are migrated. Each interface is properly recovered (see green arrows in Fig. 3(b)). Note that only 15 plane-wave responses and 15 migrations steps were required to produce each image in Fig. 3.

## Conclusions

We have shown that recent advances in data domain Marchenko methods can be extended to incorporate plane-wave source concepts. Whereas previous data domain Marchenko methods are applied to point source gathers and therefore tend to be rather expensive for large datasets, the proposed

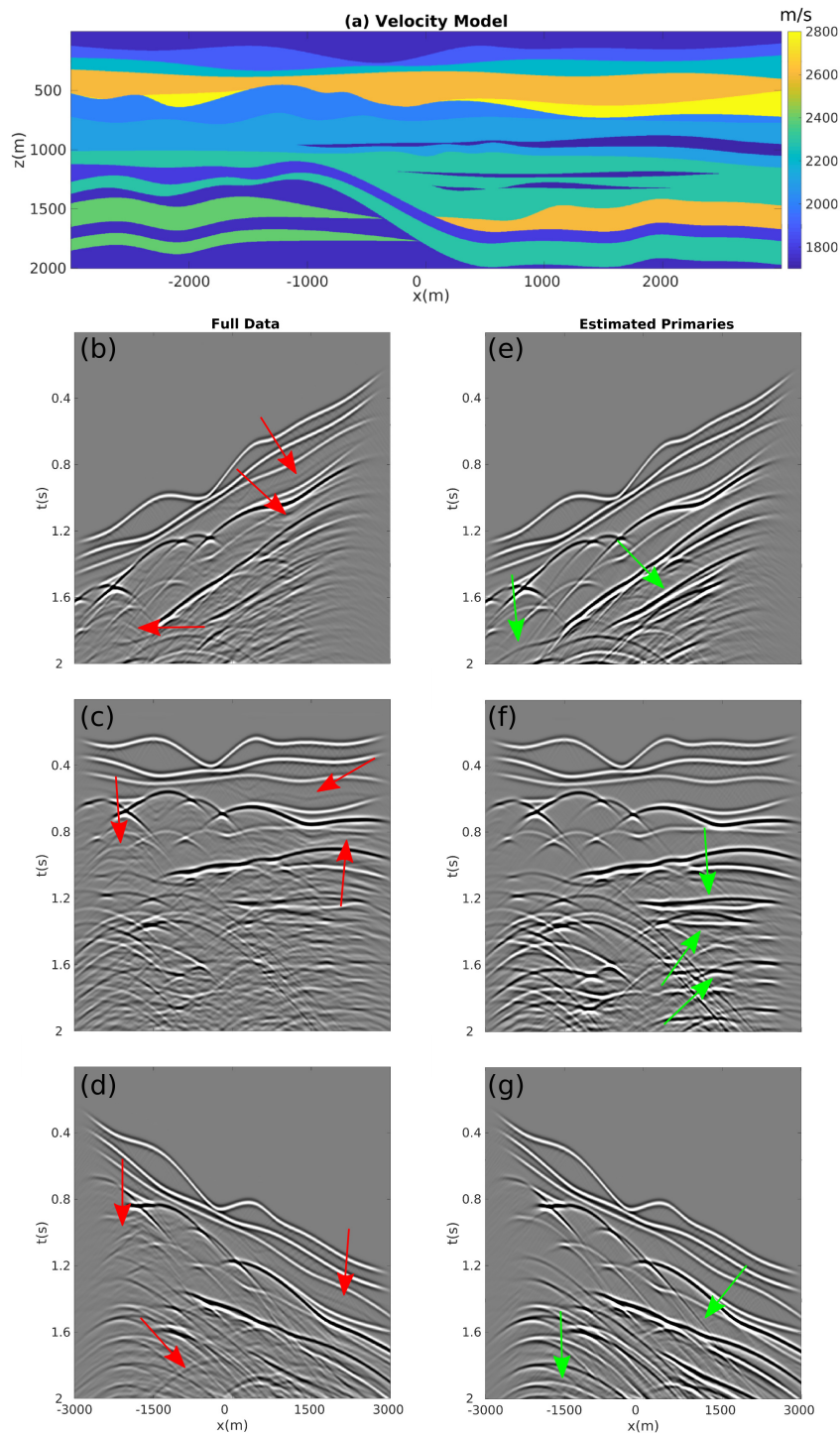


**Figure 2** (a) Velocity model used in the numerical experiment. (b-d): reflection responses associated with plane wave sources at  $-15^\circ$ ,  $0^\circ$  and  $15^\circ$ , respectively. Red arrows show internal multiples. (e-g): estimated primaries associated with plane wave sources at  $-15^\circ$ ,  $0^\circ$  and  $15^\circ$ , respectively. Differences in amplitude between gathers in (b-d) and (e-g) are due to multiples removal and transmission loss compensation. Green arrows show primaries barely visible in the corresponding full datasets (b-d).

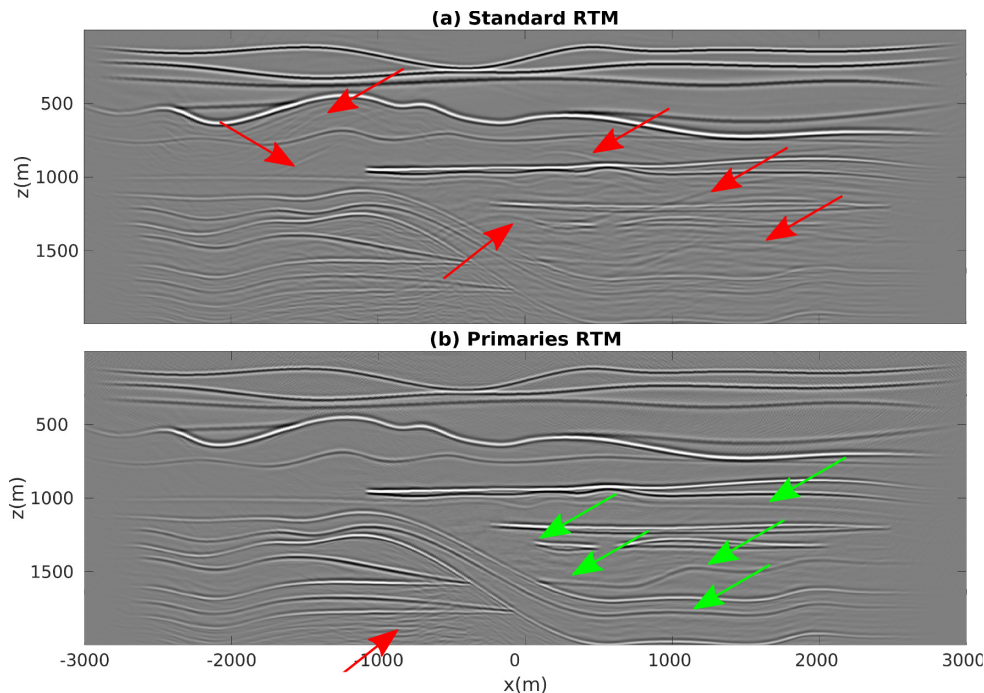


**Figure 3** (a) Aggregate RTM of 15 plane wave full datasets (uniformly ranging from  $-35^\circ$  to  $35^\circ$ ). Red arrows point at artefacts related to internal multiples. (b) Aggregate Standard RTM of synthesized primaries retrieved using Eqs. 7 and 8. Green and red arrows indicate interfaces barely visible in (a) and minor residual artefacts, respectively. Differences in amplitude between (a) and (b) are due to multiples removal and transmission loss compensation (see Fig. 2).

method only involves one primary synthesis step and a single migration per plane-wave input datasets. The plane-wave source primary synthesis algorithm discussed in this paper could then be used as an initial and unexpensive processing step, potentially guiding more expensive target imaging techniques. Here we have discussed 2D examples and internal multiples, but an obvious extension would allow surface source primary synthesis in 3D problems as well as incorporating free surface multiples.

### Acknowledgements

This work is partly funded by the European Research Council (ERC) under the European Union's Horizon 2020 research and innovation programme (grant agreement No: 742703).

### References

- Meles, G.A., Wapenaar, K. and Thorbecke, J. [2018] Virtual plane-wave imaging via Marchenko redatuming. *Geophysical Journal International*, **214**(1), 508–519.
- van der Neut, J. and Wapenaar, K. [2016] Adaptive overburden elimination with the multidimensional Marchenko equation. *Geophysics*, **81**(5), T265–T284.
- Ravasi, M., Vasconcelos, I., Kritski, A., Curtis, A., Filho, C.A.d.C. and Meles, G.A. [2016] Target-oriented Marchenko imaging of a North Sea field. *Geophysical Supplements to the Monthly Notices of the Royal Astronomical Society*, **205**(1), 99–104.
- Staring, M., Pereira, R., Douma, H., van der Neut, J. and Wapenaar, K. [2018] Source-receiver Marchenko redatuming on field data using an adaptive double-focusing method. *Geophysics*, **83**(6), S579–S590.
- Wapenaar, K., Thorbecke, J., van der Neut, J., Brogгинi, F., Slob, E. and Snieder, R. [2014] Marchenko imaging. *Geophysics*, **79**(3), WA39–WA57.
- Zhang, L. and Slob, E. [2020] A field data example of Marchenko multiple elimination. *Geophysics*, **85**(2), S65–S70.
- Zhang, L., Thorbecke, J., Wapenaar, K. and Slob, E. [2019] Transmission compensated primary reflection retrieval in data domain and consequences for imaging. *Geophysics*, **84**(4), Q27–Q36.